BASIC CONCEPTS I

H. Klein
Institut für Angewandte Physik der J.W. Goethe-Universität, Frankfurt am Main, Germany

ABSTRACT

In a simple rf system of a source, a transmission line and a cavity acting as a load, the first concern of the systems engineer would be to match the elements for maximum efficiency. This problem is discussed using transmission line theory. Quarter-wave matching and techniques for measuring mismatches and terminal impedances are described. The characteristics of cavities and techniques for their measurement are also covered with special reference to the types of cavities used in particle accelerators.

1. TRANSMISSION LINE

Transmission lines are widely used in high-frequency applications. In general they comprise two conductors separated by a dielectric e.g. a co-axial line, parallel plates, twin feeders, shielded pairs, etc. An analysis can be based on lumped-circuit parameters, or differential equations can be derived from Maxwell's equations. In the analysis below, counter-flowing currents are considered in the two conductors under the influence of distributed, series inductors and shunt capacitors between the conductors. First a lossless line is considered and then one with attenuation. A complete analogy also exists with wave propagation in waveguides ($E \equiv V$, $H \equiv I$).

1.1 Line without attenuation

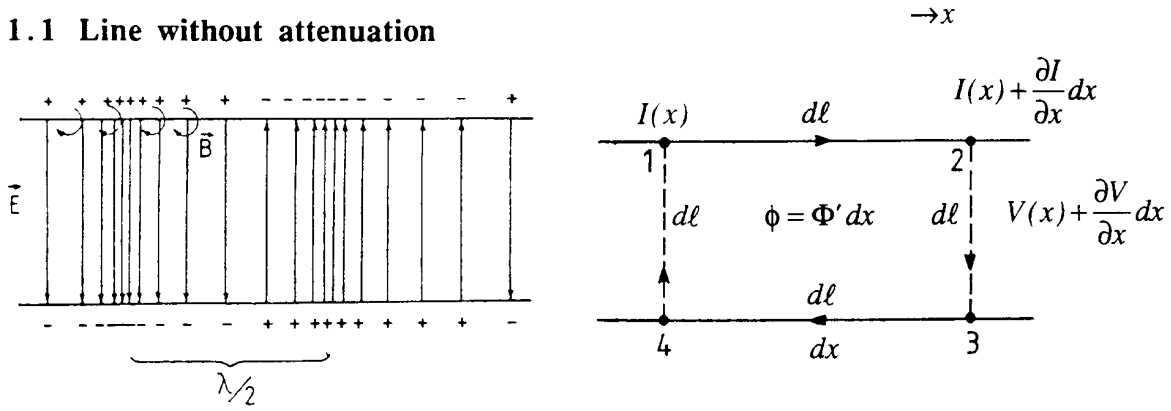

(a) (b)

Fig. 1 Transmission line without attenuation

Consider the application of Faraday's law to the loop 1-2-3-4 shown in Fig. 1(b) formed by an elementary length dx of transmission line. When there are no losses

$$\oint \vec{E} \cdot d\vec{\ell} = V(x) + \frac{\partial V(x)}{\partial x}\, dx - V(x) = \frac{\partial V(x)}{\partial x}\, dx = -\frac{\partial \Phi}{\partial t} \tag{1}$$

where Φ is the magnetic flux within the loop due to the currents in the lines. Let a prime indicate the value per length of a distributed parameter so that $\Phi' = L'I$ where L' is the inductance per length. Substitution in (1) gives

$$\frac{\partial V(x)}{\partial x} dx = -L' \frac{\partial I}{\partial t} dx \quad , \text{ which simplifies to } \quad \frac{\partial V}{\partial x} = -L' \frac{\partial I}{\partial t} \, . \tag{2}$$

The charge q' stored per length by the distributed capacitance C' will be

$$q' = C'V \ . \tag{3}$$

Thus over a distance dx, and with the use of the continuity equation

$$\frac{\partial q'}{\partial x}\, dx = \frac{\partial}{\partial t}(C'V)\, dx$$

$$-\frac{\partial I}{\partial x}\, dt = C'\, \frac{\partial V}{\partial t} dx$$

$$\frac{\partial I}{\partial x} = -C'\, \frac{\partial V}{\partial t} \ . \tag{4}$$

Differentiation of the line equations (2) and (4) gives

$$\frac{\partial^2 I}{\partial x^2} = L'C' \frac{\partial^2 I}{\partial t^2} = \frac{1}{v_{ph}^2} \frac{\partial^2 I}{\partial t^2} \tag{5}$$

$$\frac{\partial^2 V}{\partial x^2} = L'C' \frac{\partial^2 V}{\partial t^2} = \frac{1}{v_{ph}^2} \frac{\partial^2 V}{\partial t^2} \tag{6}$$

where $v_{ph} = (L'C')^{-1/2}$. The solutions of (5) and (6) are well-known and can be seen to be special cases of the general solutions given in the next section (7) and (8) and v_{ph} will be seen to be the phase velocity of the wave on the line.

1.2 Line including attenuation

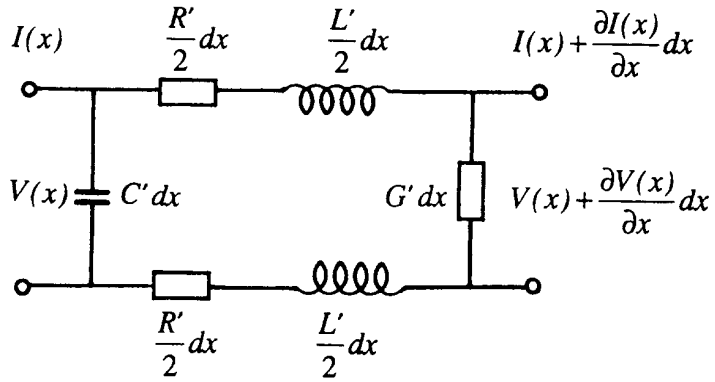

Fig. 2 Transmission line with attenuation

Let G' be the transverse conductivity per length, and R' the resistance per length. Faraday's Law can be applied to an elementary section of line, as in the previous section to give more general formulations of (2) and (4). Hence,

$$\frac{\partial V}{\partial x} = -L'\frac{\partial I}{\partial t} - R'I \tag{2a}$$

$$\frac{\partial I}{\partial x} = -C'\frac{\partial V}{\partial t} - G'V \tag{4a}$$

which leads to

$$\frac{\partial^2 V}{\partial x^2} = L'C'\frac{\partial^2 V}{\partial t^2} + (C'R' + L'G')\frac{\partial V}{\partial t} + G'R'V \ . \tag{6a}$$

Substitution of the trial solution $V = V_0\, e^{i\omega t - \gamma x}$ yields,

$$\gamma = \pm\sqrt{(R' + i\omega L')(G' + i\omega C')}, \qquad \text{(Propagation constant)} \tag{7}$$

which can be split into real and imaginary parts to give,

$$\begin{aligned} &\gamma = \alpha + ik \\ &\alpha = \pm\sqrt{0.5(G'R' - \omega^2 L'C') + 0.5\sqrt{(R'^2 + \omega^2 L'^2)(G'^2 + \omega^2 C'^2)}} \\ &k = \pm\sqrt{0.5(\omega^2 L'C' - G'R') + 0.5\sqrt{(R'^2 + \omega^2 C'^2)(G'^2 + \omega^2 C'^2)}} \end{aligned} \tag{8}$$

so that

$$V(x,t) = V_1 e^{-\alpha x} e^{i(\omega t - kx)} + V_2 e^{\alpha x} e^{i(\omega t + kx)} \ . \tag{9}$$

This solution is a superposition of forward and backward travelling waves of frequency ω with attenuation α. The amplitudes V_1 and V_2 are complex (phasors) in order to account for the initial phase of the waves. The phase and group velocities and wavelength, v_{ph}, v_g and λ, are related in the usual way by,

$$v_{ph} = \frac{\omega}{k}, \quad v_g = \frac{d\omega}{dk}, \quad \lambda = \frac{2\pi}{k} \ . \tag{10}$$

The corresponding solution for the current is found by substituting $V(x,t)$ into (4a):

$$I(x,t) = \frac{V_1}{Z_o} \cdot e^{-\alpha x} \cdot e^{i(\omega t - kx)} - \frac{V_2}{Z_o} \cdot e^{\alpha x} \cdot e^{i(\omega t + kx)} \ . \tag{11}$$

The characteristic impedance of the line is called Z_0 and is given by,

$$Z_o = \frac{V_1}{I_1} = -\frac{V_2}{I_2} = \sqrt{\frac{R' + i\omega L'}{G' + i\omega C'}} \ . \tag{12}$$

In general Z_O will vary with frequency so that $Z_O = Z_O(\omega)$ and $k = k(\omega)$, that is losses lead to dispersion!

For the special case of the lossless line $G' = R' = 0$, so that

$$v_{ph} = \frac{1}{\sqrt{L'C'}}, \quad v_g = \frac{d\omega}{dk} = v_{ph} \tag{10a}$$

$$Z_o = \sqrt{\frac{L'}{C'}}, \qquad \gamma = i\omega\sqrt{L'C'} = ik \ . \tag{12a}$$

and (9) and (11) become the main equations, which will be used in the following sections,

$$V(x,t) = V_1 e^{i(\omega t - kx)} + V_2 e^{i(\omega t + kx)} \tag{13}$$

$$I(x,t) = \frac{V_1}{Z_o} e^{i(\omega t - kx)} - \frac{V_2}{Z_o} e^{i(\omega t + kx)} . \tag{14}$$

1.3 Line terminated by a load

In all that follows a lossless line will be considered and the time variation $e^{i\omega t}$ will be omitted since it appears equally in all terms.

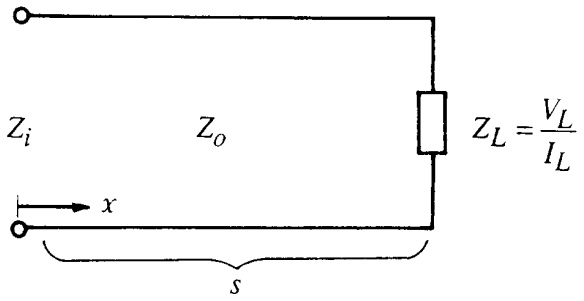

Fig. 3 Transmission line terminated by a load

When a line has a terminal load impedance Z_L a boundary condition can be established by summing the forward and backward wave voltages and currents at the terminal load ($x = s$), dividing them and equating the result to the terminal impedance Z_L.

$$V(s) = V_L = V_1 e^{-iks} + V_2 e^{iks} = V^+ + V^- \tag{15}$$

$$I(s) = I_L = \frac{V^+}{Z_o} - \frac{V^-}{Z_o} \,. \tag{16}$$

Since $V_L = Z_L I_L$

$$V^+ = \frac{1}{2} V_L (1 + \frac{Z_o}{Z_L}) \quad \text{and} \quad V^- = \frac{1}{2} V_L (1 - \frac{Z_o}{Z_L}) \,. \tag{17}$$

A reflection factor ρ is defined at the load in terms of the forward and backward waves and this can then be related to the terminating impedance by (17), so that,

$$\rho = \frac{V^-}{V^+} = \frac{V_2}{V_1} e^{2iks} = \frac{Z_L - Z_o}{Z_L + Z_o} \,. \tag{18}$$

A corresponding transmission coefficient can also be defined. By measuring the complex reflection coefficient ρ, the complex Z_L can be found. It is useful to note some particular cases:

(a) Short-circuited line: $Z_L = 0$, $|\rho| = 1$, $\phi = \pi$ (phase shift between V_1 and V_2)

$$\begin{aligned} V(x) &= 2V^+ e^{i\pi/2} \cos(k(x-s) + \pi/2) = 2iV^+ \sin[k(s-x)] \\ I(x) &= 2\frac{V^+}{Z_o} \cos(k(x-s)) \end{aligned} \tag{19}$$

which represent a standing wave with a phase shift between V and I of $\pi/2$ in space and time.

(b) Open-circuit line: $Z_L = \infty$, $|\rho| = 1$, $\phi = 0$

$$V(x) = 2V^+ cos(k(x-s))$$
$$I(x) = 2\frac{V^+}{Z_o}e^{i\pi/2} cos(k(x-s)+\pi/2) = 2i\frac{V^+}{Z_0} sin[k(s-x)] \ . \tag{20}$$

(c) Matched line: $Z_L = Z_O$, $\rho = 0$, $\phi = 0$

$$V(x) = V^+ e^{-ik(x-s)}$$
$$I(x) = \frac{V^+}{Z_o} e^{-ik(x-s)} \ . \tag{21}$$

(d) Behaviour of mismatched lines. Consider $Z_L = nZ_O$, $\rho = \frac{n-1}{n+1}$. (n ≥ 0).

For $n > 1$ the reflection coefficient will be $\rho > 0$ and $\phi = 0$, and as n increases $\rho \rightarrow 1$.
For $n < 1$ the reflection coefficient will be $\rho < 0$, $\phi = \pi$, and as n decreases $\rho \rightarrow -1$.

1.4 Input impedance

The input impedance, Z_i, is given by:

$$Z_i = \frac{V_1(x=0)}{I_1(x=0)} \text{ which after some manipulation yields } Z_i = Z_o \frac{Z_L + iZ_o tan(ks)}{Z_o + iZ_L tan(ks)} \tag{22}$$

Thus the complex impedance, seen at the input depends on the load Z_L and the line length s. Again it is useful to note some particular cases.

(a) Half-wavelength line

Consider a line of one half wavelength, then $s = \lambda/2$ and from (22) $Z_i = Z_L$. In this special case, the input impedance equals the load, independent of the line impedance Z_0 (remembering $k = 2\pi/\lambda$).

(b) Quarter-wavelength line

Consider a line of one quarter wavelength, then $s = \lambda/4$ and from (22),

$$Z_i = \frac{Z_o^2}{Z_L} \quad \text{(Quarter – wave transformer)} \tag{23}$$

Equation (23) provides a useful way of matching two impedances by adapting the line between them. This is best illustrated by an example. Consider the problem of matching a 60 Ω source to 100 Ω load using a 'quarter wave transformer' as shown in Fig. 4.. To ensure a match the required inter-line impedance is given by (23) and is $Z_o = (60 \times 100)^{1/2} = 77.5\ \Omega$. Note that the sum of all reflections is equal to zero, but this is only correct for one frequency. In the case of pulses, a match is not possible, since a pulse contains a very wide spread in frequencies. This can be seen from the Fourier expansion for a pulse. But since the reflection coefficient ρ is valid for all frequencies, it is valid also for a pulse. Therefore reflection and transmission of pulses can easily be calculated. As an example, the behaviour of a pulse fed into the matching

transformer (Fig. 4) is considered (Fig. 5). As pulse [1]→ arrives at the discontinuity ($Z_1 = 60$ → $Z_0 = 77\ \Omega$), it is split into a reflected pulse ←[1] and a transmitted pulse [2]→ and so on; since [3]→ is matched, there will be no reflection; [4]→ and ←[4] – with a phase jump of π – belong to the reflected pulse ←[2], and an infinite series of reflections occurs with decreasing pulse amplitudes.

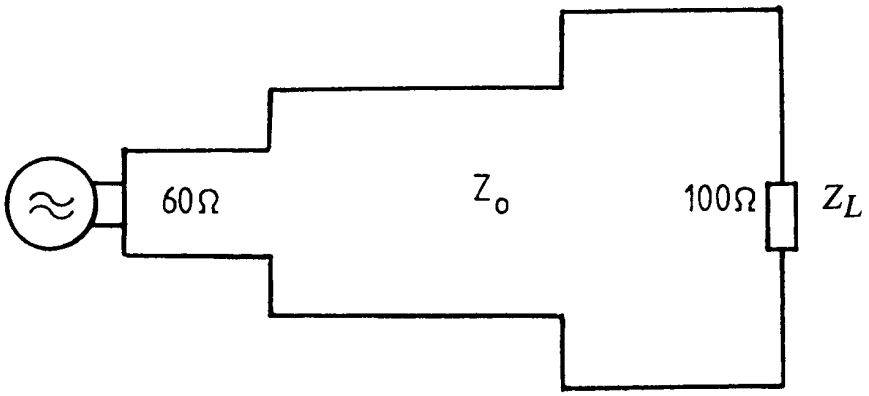

Fig. 4 Impedance matching transformer

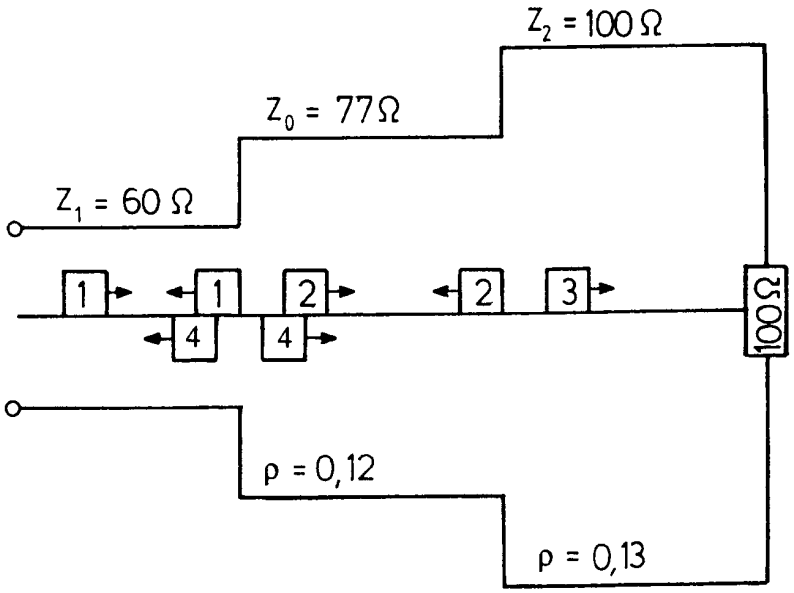

Fig. 5 Reflection of pulses in the impedance matching transformer

The application of (18) to the different boundaries in Fig. 5 gives numerically,

$$\vec{V}_1 = 1,\ \rho_1 = 0.127,\ \rho_2 = 0.127$$
$$\vec{V}_1 = \rho_1 \vec{V}_1 = 0.127$$

where the 'vector arrow' denotes the direction of the pulse propagation. The energy in a pulse is proportional to V^2:

$$\vec{V}_2 = \sqrt{\vec{V}_1^2 - \tilde{V}_1^2} = 0.992$$

$$\tilde{V}_2 = \rho_2 \vec{V}_2 = 0.126$$

$$\vec{V}_3 = 0.984$$

$$\tilde{V}_4 = 0.125$$

$$\vec{V}_4 = 0.016$$

1.5 Measuring mismatches

In section 1.3, the effect of terminating a line with a load impedance was discussed with the help of a complex reflection coefficient defined in (18). The reflected wave and the forward wave interfere and the standing wave pattern thus created can be detected and used to measure the mismatch. The ratio of the maximum voltage to the minimum voltage in the standing wave is known as the Voltage Standing Wave Ratio (VSWR) and is denoted S_W. Note the inclusion of modulus signs in the definition of the VSWR. These are needed because the measurement techniques will average over time and the amplitudes of the voltages will be detected. The maximum voltage will occur at a point where the forward and backward waves have the same phase so that their amplitudes add directly. Similarly, the minimum voltage will occur at a phase where they are opposed.

$$S_W = \frac{V_{max}}{V_{min}} = \frac{|V_1| + |V_2|}{|V_1| - |V_2|} \quad (= \text{VSWR}) \tag{24}$$

Some methods for measuring S_W, ρ and Z_L are presented in this section. For these measurements the use of waveguides rather than transmission lines does not affect the results or procedures.

1.5.1 Slotted line with movable probe

Figure 6 shows an rf generator feeding a cavity with a slotted line in the input. A movable probe measures the voltage at different positions along the standing wave and thus measures the VSWR due to any mismatch.

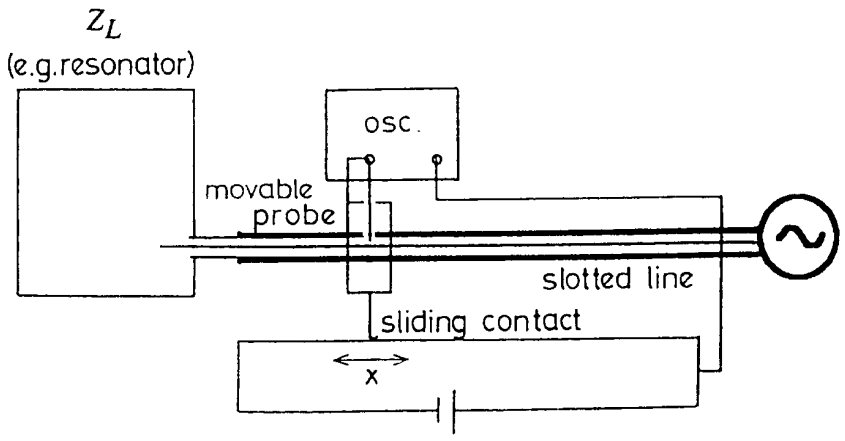

Fig. 6 Voltage Standing Wave Ratio (VSWR) measurements with a slotted line

The combination of (18) and (24) gives

$$|\rho| = \frac{S_W - 1}{S_W + 1} = \frac{|Z_L - Z_o|}{|Z_L + Z_o|} \quad . \tag{25}$$

The inversion of (25) gives

$$Z_L = Z_o \frac{1+\rho}{1-\rho} \quad . \tag{26}$$

Thus the reflection factor $|\rho|$ and the terminal load impedance $|Z_L|$ is obtained from (25) and (26). The position of the probe then gives the phase $Z_L = |Z_L|e^{i\phi}$. The measurement of λ is simple since the distance between two minima = $\lambda/2$.

1.5.2 Four Fixed Probes with display of ρ

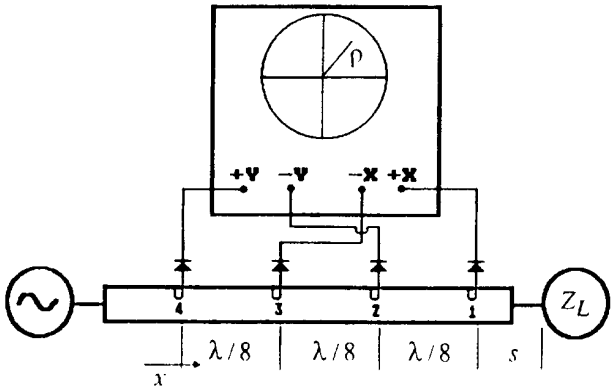

Fig. 7 Four-Fixed-Probe technique (less used nowadays)

In this case, the movable probe is replaced by four fixed probes and the outputs are conveniently displayed as the complex reflection coefficient in polar form (see Fig. 7). Although this technique has been largely superseded by more sophisticated electronic equipment such as scalar and vectorial network analyzers, it is a clear illustration of the underlying theory.

Consider a transmission line of length s, terminated with a load of reflection coefficient ρ as shown in Fig. 3. The expression for the voltage on this line, without the time variation, is obtained from (13)

$$V(x) = V_1 e^{-ikx} + V_2 e^{ikx} \quad . \tag{14a}$$

Let the load have a complex reflection coefficient at the load of $\rho = |\rho|e^{i\phi}$, then by (18)

$$\rho = |\rho|e^{i\phi} = \frac{V_2}{V_1} e^{2iks} \quad . \tag{27}$$

Consider now the instrument in Fig. 7. Let the distance from the load to the first probe be s and place the origin x=0 at this point. The voltage at probe 1 would then simply be

$$V_{\text{probe 1}} = V_1 + V_2 = V_1(1 + V_2 / V_1)$$

and with (27) would become

$$V_{\text{probe 1}} = V_1(1 + |\rho|e^{i(\phi - 2iks)}) \quad . \tag{28}$$

The probe, however, only detects the amplitude, so the square of the modulus of (28) is taken

$$|V_{\text{probe }1}|^2 = |V_1|^2(1+|\rho|^2+2|\rho|\cos(2ks-\phi)) \ . \tag{29}$$

Exactly the same analysis can be applied to all the probes. Although V_1 will have different phases for each probe $|V_1|$ will be the same. For each probe the distance s is increased by $\lambda/8$, that is the argument of the cosine is increased by $\pi/2$. Thus,

$$\begin{aligned} |V_{\text{probe }2}|^2 &= |V_1|^2(1+|\rho|^2+2|\rho|\sin(2kd-\phi)) \\ |V_{\text{probe }3}|^2 &= |V_1|^2(1+|\rho|^2-2|\rho|\cos(2kd-\phi)) \\ |V_{\text{probe }4}|^2 &= |V_1|^2(1+|\rho|^2-2|\rho|\sin(2ks-\phi)) \ . \end{aligned} \tag{30}$$

For $|V_{\text{probe }1}|^2 - |V_{\text{probe }3}|^2$ and $|V_{\text{probe }2}|^2 - |V_{\text{probe }4}|^2$ it follows that

$$|V_{\text{probe }1}|^2 - |V_{\text{probe }3}|^2 = |V_1|^2 4|\rho|\cos(2ks-\phi) \tag{31}$$

$$|V_{\text{probe }2}|^2 - |V_{\text{probe }4}|^2 = |V_1|^2 4|\rho|\sin(2ks-\phi) \ . \tag{32}$$

Equations (31) and (32) represent ρ in polar coordinates. A simple arrangement using diodes with a square-law response (small amplitudes) makes it possible to display the reflection coefficient on an X-Y oscilloscope.

1.5.3 Directional coupler method

Direct measurement of ρ and ϕ can be made by two directional couplers (see Fig. 8)

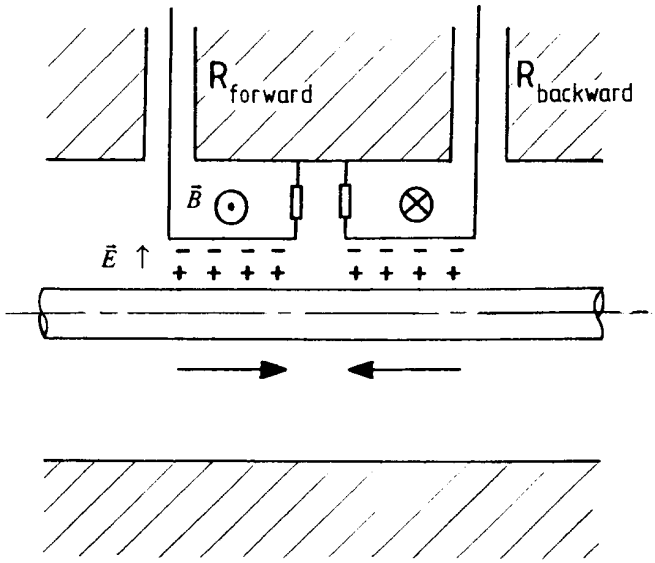

Fig. 8 Double directional-coupler reflectometer

The dimensions of the loop and the resistor have to be chosen such that the currents induced by the magnetic and the electric field respectively have the same value. Due to the orientation of the loop, the currents either add up or cancel each other corresponding to the forward or backward travelling wave. So the reflection coefficient can be measured singly by two directional couplers forming a directional bridge.

Since the coaxial line (see Fig. 9) is one of the most important transmission lines, some characteristic parameters are given.

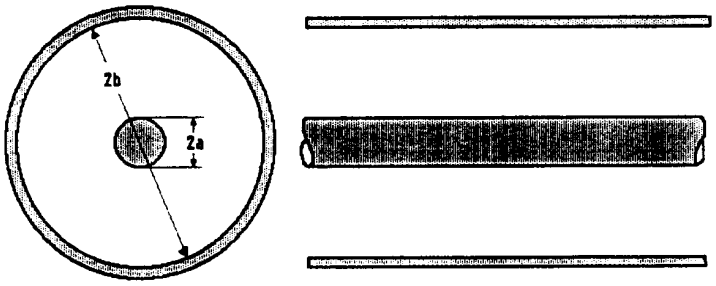

Fig. 9 Geometry of a coaxial transmission line

The inductance per length is given by $L'=\Phi' I$, which can be evaluated from the magnetic field between the two conductors.

$$\oint \vec{H}\cdot d\vec{\ell} = I \ , \quad \text{so that} \quad B=\frac{\mu I}{2\pi r} \ .$$

The total flux linking the inner conductor per unit length is then

$$\Phi' = \int_a^b B \ dA' = \int_a^b B \ dr = I\frac{\mu}{2\pi} ln\frac{b}{a}$$

where A' is the area in the radial-longitudinal plane between the inner and outer conductors. Thus the inductance per length is,

$$L' = \frac{\mu}{2\pi} ln\frac{b}{a} \ . \tag{33}$$

Similarly the capacitance per length can be found from

$$C' = \frac{q'}{\int_a^b E_r \ dr} = \frac{q'}{\int_a^b \frac{1}{2\pi\varepsilon} q' \frac{1}{r} dr} = \frac{2\pi\varepsilon}{ln\frac{b}{a}} \ . \tag{34}$$

The substitution of (33) and (34) into (10a) leads to,

$$L'C' = \mu\varepsilon = \frac{1}{v_{ph}^2} \ . \tag{35}$$

For a vacuum-filled line, $\mu = \mu_o$ and $\varepsilon = \varepsilon_o$, then by (35) $v_{ph} = c$ where c is the speed of light. For dielectric-filled lines the phase velocity is slowed down. For example, with poly-ethylene $\mu_r = 1$, $\varepsilon_r = 2.26$, then by (35) $v_{ph} = \frac{c}{1.5}$.

Substitution into (12a) gives the characteristic impedance Z_0 of the line,

$$Z_o = \frac{V}{I} = \frac{|E|}{|H|} = \sqrt{\frac{L'}{C'}} = \frac{ln\frac{b}{a}}{2\pi}\sqrt{\frac{\mu}{\varepsilon}} \quad . \tag{36}$$

Equation (36) can be rewritten using the impedance of free space $\sqrt{(\mu_0 / \varepsilon_0)} = 120\pi$ [ohm]

$$Z_o = \frac{ln\frac{b}{a}}{2\pi}\sqrt{\frac{\mu_r}{\varepsilon_r}}\ 120\pi \text{ [ohm]} \ .$$

The power flow density [watt/m^2] in the line is given by Poynting's vector:

$$\vec{S} = \vec{E} \times \vec{H} = \frac{q'}{2\pi\varepsilon r}\ \frac{I}{2\pi r} \ .$$

Since $q'=C'V$ and C' is given by (34), this becomes

$$S = \frac{VI}{2\pi}\ \frac{1}{ln\frac{b}{a}}\ \frac{1}{r^2} \ .$$

After integration over the cross-sectional area of the line the total power flow is,

$$S_o = \int \vec{S} \cdot d\vec{A} \ = \frac{VI}{2\pi ln\frac{b}{a}} \int_a^b \frac{1}{r^2} 2\pi r \ dr = VI \ \text{ or } \ \bar{S}_o = V_{eff}\ I_{eff} \ . \tag{37}$$

2. THE QUALITY FACTOR Q OF A RESONATOR (FIGURE OF MERIT)

The design of cavity resonators, as they are commonly used for particle accelerators, determines their efficiency at concentrating the field in the region of the beam, storing energy, having the correct resonant frequency and so on. The most important characteristic number for a cavity is its 'quality factor', Q, which is defined as,

$$Q = \frac{2\pi \ \text{stored energy}}{\text{energy consumed per period}} = \frac{2\pi U}{TW} = \frac{\omega_o U}{W} \tag{38}$$

where U is the stored energy, W is the average rate of energy loss, T is the period of oscillation and ω_0 is the natural resonant frequency. If the resonator is unloaded $Q=Q_0$ and W is the power lost in cavity, but if the resonator is open and loaded $Q = Q_L$ and W is the power lost in cavity and the external system (feeding line, transmitter etc.).

2.1 Closed, free-running cavity

In a closed cavity, the power loss will be equal to the rate of change of the stored energy,

$$W = -\frac{dU}{dt} \ \text{ and from (38) } \ W = \frac{\omega_0}{Q} U$$

so that the decay of the stored energy will be

$$W = W_o e^{-t/\tau_W} \tag{39}$$

where

$$\tau_W = \frac{Q}{\omega_o} = \text{decay time of stored energy} . \tag{40}$$

Since $W \propto E^2$, the field will decay as

$$E(t) = E_O \; e^{-\frac{t}{2\tau_W}} \; e^{i\omega t} \tag{41}$$

where

$$\tau_E = \frac{2Q}{\omega_o} = 2\tau_W \quad \text{decay time of field} . \tag{42}$$

The homogeneous differential equation for an oscillator with damping factor p is

$$\frac{d^2E}{dt^2} + p\frac{dE}{dt} + \omega_{oo}^2 E = 0 . \tag{43}$$

where ω_{00} is the resonant frequency when $p = 0$. Substitution of the trial solution

$$E = E_0 e^{\lambda t} \text{ leads to } \lambda^2 + p\lambda + {\omega_{00}}^2 = 0$$

yields

$$\lambda = -\frac{p}{2} \pm i\sqrt{{\omega_{00}}^2 - (p/2)^2} = -\frac{p}{2} \pm i\omega_0 .$$

For $\omega_{oo}^2 > \left(\frac{p}{2}\right)^2$, the solution will be harmonic with an exponential envelope. Thus the decay of the field will be given by

$$E = E_o \; e^{-(p/2)t} \; e^{i\omega_o t} = E_o \; e^{-t/\tau_E} \; e^{i\omega_o t} \tag{44}$$

and by comparison with (41) and (42), it can be seen that,

$$\tau_E = \frac{2}{p} = \frac{2Q}{\omega_o} \text{ and that } p = \frac{\omega_o}{Q} . \tag{45}$$

2.2 Cavity with external excitation

With an external excitation force $C\, e^{i\omega t}$ (43) becomes

$$\frac{d^2E}{dt^2} + p\frac{dE}{dt} + \omega_{oo}^2 E = Ce^{i\omega t} . \tag{46}$$

Substitution of the trial solution $E=A\, e^{i\omega t}$ gives

$$A = \frac{C}{\left(\omega_{oo}^2 - \omega^2\right) + i\omega p} = \frac{C}{\left(\omega_{oo}^2 - \omega^2\right) + i\frac{\omega\omega_{oo}}{Q}} . \tag{47}$$

From (47) it can be seen that, as $\omega \to 0$ then $A \to \frac{C}{\omega_\infty^2}$ and as $\omega \to \infty$ then $A \to 0$.

When the external frequency is close to the natural frequency then,

$$\omega_o^2 - \omega^2 = (\omega_o - \omega)(\omega_o + \omega) \approx 2\omega_o \Delta\omega$$

$$A = \frac{C}{2\omega_o \Delta\omega + i\frac{\omega_0^2}{Q}} . \tag{48}$$

Thus $|A|$ is maximum when $\Delta\omega$ is zero, that is the cavity is tuned to the resonant frequency. In this case

$$A = \frac{CQ}{i\omega_o^2} \text{ and } |A|_{max} = \frac{CQ}{\omega_0^2} .$$

The phase difference between A and C is described by $-i$,which is $-\pi/2$. The stored energy is proportional to the square of the amplitude of the field so that,

$$U \propto |A^2| = \frac{C^2 / 4\omega_o^2}{\Delta\omega^2 + \frac{\omega_0^2}{4Q^2}} \propto \frac{1}{\Delta\omega^2 + \left(\frac{\omega_0}{2Q}\right)^2} \tag{49}$$

The quality of the resonator may be characterised by the 'narrowness' of its resonance. Let $\Delta\omega_H$ be the full width at half height of the $|A^2|$ versus ω–curve (i.e. stored energy versus excitation frequency, see Fig. 10), so that

$$|A^2| = \frac{|A_{max}^2|}{2} : \text{ when } \Delta\omega = \pm\frac{1}{2}\Delta\omega_H$$

then by (49)

$$\Delta\omega_H = \frac{\omega_0}{Q} \text{ , or } Q = \frac{\omega_0}{\Delta\omega_H} = \frac{f}{\Delta f_H} . \tag{50}$$

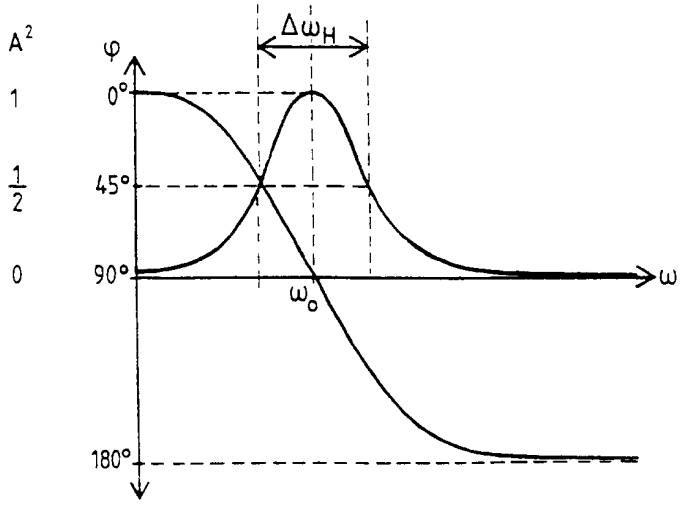

φ = phase angle between C and A:

Fig. 10 Stored energy and phase shift with respect to the excitation of a resonator

Thus for $\omega=\omega_0 \pm\Delta\omega_H/2$ the amplitude A has decreased to $A/\sqrt{2}$ and the stored energy is reduced by 1/2. From (50) it is clear that Q is a measure of the 'narrowness' of the resonance (that is of the curve of stored energy against excitation frequency) and is therefore a measure of the quality of the cavity.

Equation (47) relates the two amplitudes A and C. The phase shift between these amplitudes can be found from the denominator of (47) and is given by

$$tan\varphi = -\frac{\omega\omega_o / Q}{\omega_o^2 - \omega^2} . \tag{51}$$

Thus (51) shows that when

$$\begin{aligned} &\omega = 0 \quad && tan\varphi = 0 \quad && \varphi = 0 \\ &\omega = \infty \quad && tan\varphi = 0 \quad && \varphi = -\pi \\ &\omega = \omega_0 \quad && tan\varphi = \infty \quad && \varphi = -\pi/2 . \end{aligned}$$

For a given phase shift (51) can be solved to give,

$$\frac{\omega}{\omega_0}(\varphi) = -\frac{1}{2Q tan\varphi} + \sqrt{1+\left(\frac{1}{2Q tan\varphi}\right)^2} \tag{52}$$

If (51) is evaluated for the phase shifts $\varphi = \pm\pi/4$, then

$$\pm 1 = \frac{\omega\omega_0}{Q(\omega_0^2 - \omega^2)} \approx \frac{\omega_0}{2Q\Delta\omega} \quad \text{which gives} \quad \Delta\omega = \pm\frac{\omega_0}{2Q} .$$

By comparison with (50), it can be seen that $\Delta\omega$ is just half $\Delta\omega_H$ and that the phase shifts $\varphi = \pm\pi/4$ correspond to the half height of the curve.

For small angles

$$tan\Delta\varphi \approx Q\frac{2\Delta\omega}{\omega} \quad \text{so that} \quad \frac{\Delta\varphi}{\Delta\omega} = \frac{2Q}{\omega} . \tag{53}$$

2.3 Measurement of Q

There are several methods which can be used to measure Q based on the information given in the two previous sections.

(i) In a closed resonator the decay time of the stored energy from (40) gives $Q = \omega_0 \tau_W = Q_o$,or the decay of the amplitude of E or H: from (45) gives $Q = \omega_0 \tau_E/2 = Q_o$. For example, for a conventional cavity $\omega_0 = 2\pi\ 500\ 10^6$ Hz, Q = 10000 gives a decay time of $\tau_W \approx 3\mu s$! For a superconducting cavity:$Q = 10^8$ and gives a decay time of $\tau_W \approx 30ms$

(ii) Measurement of $\Delta\omega$ when the stored energy is halved, which corresponds to a signal drop of -3.01 dB, can be used with (50) to give,

$$Q = \frac{\omega_o}{\Delta\omega_H}$$

or alternatively $\Delta\omega_H$ can be found by detecting the phase shifts of $\Delta\phi = \pm 45°$.

3. Measurement of $\Delta\varphi/\Delta\omega$ in the neighbourhood of the resonance [see (53)], so

$$Q = \frac{\omega_o}{2\Delta\omega} tan\Delta\varphi \approx \frac{\omega_o}{2}\frac{\Delta\varphi}{\Delta\omega} .$$

In the last two cases, the losses should not be too high, Q not too small and the distance to neighbouring modes much greater than $\Delta\omega_H$.

2.4 Calculation of Q

From the definition of Q given in (38)

$$Q = \frac{\omega_o U}{W} \text{ , where the stored energy can be caculated from}$$

$$U = \int\left(\frac{1}{2}\varepsilon E^2 + \frac{1}{2}\mu H^2\right) dV = \int\frac{1}{2}\varepsilon\hat{E}^2(x,y,z)\ dV = \int\frac{1}{2}\mu\hat{H}^2(x,y,z)\ dV . \qquad (54)$$

The losses W can be calculated by Poynting's vector perpendicular to the surfaces via the surface currents, which are given directly by the magnetic field at the surface, that is

$$W = \int\frac{1}{2}I_{surf}^2\frac{1}{\sigma\delta}dA = \int\frac{1}{2}H_{surf}^2\frac{1}{\sigma\delta}dA \qquad (55)$$

where A = surface area, σ = conductivity and δ = skin depth. A conventional cavity uses copper, so that

$$\delta = \sqrt{\frac{2}{\mu\sigma\omega}} \text{ , for copper: } \sigma \approx 6.26\times10^7\Omega^{-1}m^{-1} \text{ , } \delta[m] \approx \frac{0.063}{\sqrt{f[Hz]}}$$

For a rectangular resonator with the dimensions a = 0.5 m, b = 0.2 m, ℓ = 0.45 m, see Fig. 11, the field distribution of the TE_{101} mode is given by:

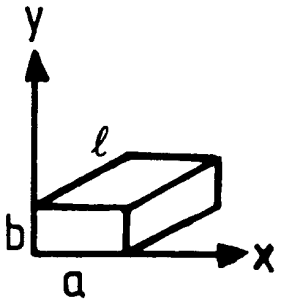

Fig. 11 Rectangular cavity

$$E_y = E_o sin(\frac{\pi x}{a})sin(\frac{\pi z}{\ell})e^{i\omega t}$$

$$H_x = -i\frac{E_o}{z_o}\frac{\lambda_o}{2\ell}sin(\frac{\pi x}{a})cos(\frac{\pi z}{\ell})e^{i\omega t}$$

$$H_z = i\frac{E_o}{z_o}\frac{\lambda_o}{2a}cos(\frac{\pi z}{\ell})sin(\frac{\pi z}{\ell})e^{i\omega t} \qquad (56)$$

$$Z_o = \sqrt{\frac{\mu_o}{\varepsilon_o}}$$

and the resonant frequency is given by

$$\omega_o = c\sqrt{\left(\frac{\pi}{a}\right)^2 + \left(\frac{\pi}{\ell}\right)^2} \quad . \tag{57}$$

It follows that $\omega_0 = 2\pi f = 2\pi$ 448 MHz and $Q \approx 33\,000$.

So far no external losses have been considered. The Q-value was given by $Q_0 = \omega_0 U/W$, where W represents the losses in the cavity. Therefore the cavity has to be loosely coupled to the transmitter, otherwise the losses W_{ext} in the transmission line and transmitter will change the result. The Q of the external system is called

$$Q_{ext} = \frac{\omega_o U}{W_{ext}} \quad . \tag{58A}$$

The loaded Q of the cavity is then:

$$Q_L = \frac{\omega_0 U}{W + W_{ext}} \tag{58B}$$

which leads to

$$\frac{1}{Q_L} = \frac{1}{Q_0} + \frac{1}{Q_{ext}} \quad . \tag{59}$$

The so-called coupling factor β is given by

$$\beta = \frac{Q_o}{Q_{ext}} = \frac{W_{ext}}{W} \tag{60}$$

and is related to the reflection coefficient at resonance by

$$|\rho| = \frac{|1 - 1/\beta|}{1 + 1/\beta} \quad . \tag{61}$$

For β=1 (so-called critical coupling) all power from the transmission line goes to the resonator and no reflection occurs. In this case

$$W_{ext} = W \ , \ \rho = 0 \quad \text{and} \quad Q_L = \frac{Q_o}{2} \quad .$$

In the case of $\beta << 1$ (weak coupling) and $\beta >> 1$ (strong coupling) all the power will be reflected.

3. RESONANT PERTURBATION MEASUREMENTS OF H AND E FIELDS

This section is based on the general theorem of Boltzmann/Ehrenfest [1-3], which states that, 'for a periodical and linear working, lossless engine the product of energy (kinetic and potential) and period time is invariant for adiabatic deformations'. This was adapted to rf cavities by Maclean [4] as

$$UT = \text{const.}$$

$$\frac{dU}{U} = -\frac{dT}{T} = \frac{d\omega}{\omega}\ , \tag{62}$$

where $\omega = 2\pi / T$. For example, in an 'LC ' oscillating circuit

$$\omega = \frac{1}{\sqrt{LC}}$$

so that for slow variation of C in time, i.e. $\Delta C/C$ very small, within one oscillating period (adiabatic change of C):

$$\frac{d\omega}{\omega} = -\frac{1}{2}\frac{dC}{C} \quad (L = \text{const.})\ . \tag{63}$$

The stored energy is given by

$$U = \frac{1}{2}CV_o^2 = \frac{1}{2}\frac{q_o^{\ 2}}{C}$$

where q_0 is the maximum charge on the capacitor andV_0 = maximum voltage on the capacitor. For an adiabatic change of C:

$$\frac{dU}{U} = -\frac{1}{2}\frac{dC}{C} \tag{64}$$

which when compared to (63) gives the original hypothesis (62)

$$\frac{d\omega}{\omega} = \frac{dU}{U}\ .$$

Increasing the separation of the plates of the capacitor requires an external force, which increases the energy of the system. Similar considerations can be made for moving a part of the surface of a resonator or for pushing a perturbating object into a cavity [5-7]. If a perturbating dielectric sphere (for the sake of simplicity) of volume v_1 is brought into the electrical field of a resonator of volume v_2, the stored energy and the resonance frequency will change. From (62)

$$\frac{\Delta\omega}{\omega_o} = \frac{\Delta U}{U_o}$$

where U_0 is the stored energy without the object and $\Delta U = U_0 - U$.

$$\Delta U = \int_0^{v_2} \frac{1}{2}\varepsilon_o E_u^2 dv - \int_{v_1}^{v_2} \varepsilon_o \left(E_u + E_{dip}\right)^2 dv - \int_0^{v_1} \frac{1}{2}\varepsilon_o \varepsilon_r E_i^2 dv \tag{65}$$

where

E_u = electrical field without the bead(E undisturbed)
E_{dip} = dipole field outside of the homogeneously polarised bead
E_i = homogeneous field inside the bead
ε_r = relative dielectric constant of the bead material.

In the quasi-static case, which is assumed here, the following relations are valid

$$E_i = \frac{3}{\varepsilon_r + 2} E_u \qquad \text{(The factor 3 stems from the depolarization factor N of a sphere, N = 1/3)}$$

$$E_{r,dip} = \frac{p\cos\vartheta}{2\pi\varepsilon_o r^3} \quad , \quad E_{\vartheta,dip} = \frac{p\sin\vartheta}{4\pi\varepsilon_o r^3}$$

$$p = \text{dipole moment} = 3v_1 \frac{\varepsilon - 1}{\varepsilon_r + 2} \varepsilon_o E_u$$

$$P = \text{polarization} \quad = \varepsilon_o \frac{3(\varepsilon_r - 1)}{\varepsilon_r + 2} E_u \ .$$

The use of these relations with the restriction of very small perturbations, that is small beads whose diameter << wavelength, it can be shown that

$$\Delta U \approx -\frac{1}{2} v_1 P E_u = -\frac{1}{2} p E_u \tag{66}$$

which is the energy of a dipole with a dipole momentum p in a homogeneous field E_u. Thus

$$\Delta U = -\frac{1}{2} v_1 \varepsilon_o \frac{3(\varepsilon_r - 1)}{\varepsilon_r + 2} E_u^2$$

and by introducing the volume of the bead

$$v_1 = \frac{4}{3}\pi r_1^3$$

$$\Delta U = -2\pi r_1^3 \varepsilon_o \frac{\varepsilon_r - 1}{(\varepsilon_r + 2)} E_u^2 \ . \tag{67}$$

On average:

$$\Delta U_{elect} = -\pi r_1^3 \ \varepsilon_o \frac{\varepsilon_r - 1}{\varepsilon_r + 2} E_{ou}^2 \ . \tag{68}$$

The corresponding result in the magnetic case is

$$\Delta U_{mag} = -\pi r_1^3 \ \mu_o \frac{\mu_r - 1}{\mu_r + 2} H_{ou}^2 \ . \tag{69}$$

The overall change in stored energy is

$$\Delta U = \Delta U_{elect} + \Delta U_{mag} \tag{70}$$

from (62), (68), (69) and (70)

$$\frac{\Delta\omega}{\omega} = \frac{\Delta U}{U} = -\frac{\pi r_1^3}{U}\left[\varepsilon_o \frac{\varepsilon_r - 1}{\varepsilon_r + 2} E_{ou}^2 + \mu_o \frac{\mu_r - 1}{\mu_r + 2} H_{ou}^2\right] . \tag{71}$$

U can be substituted by WQ/ω from (38). Q and the input power W (input = losses at equilibrium), have to be measured to get the absolute field strength, so that

$$\frac{\Delta\omega}{\omega^2} = -\frac{1}{QW}\pi r_1^3\left[\varepsilon_o\frac{\varepsilon_r - 1}{\varepsilon_r + 2}E_{ou}^2 + \mu_o\frac{\mu_r - 1}{\mu_r + 2}H_{ou}^2\right]. \tag{72}$$

Two cases are of interest:

(i) Dielectric perturbing bead

$$\mu_r = 1 \text{ , so that } \frac{\Delta\omega}{\omega} = -\frac{\pi r_1^3}{U}\varepsilon_o\frac{\varepsilon_r - 1}{\varepsilon_r + 2}E_{ou}^2 .$$

In this case, the electrical field will be measured. ΔU will be negative, since energy will be gained by introducing the ball into the field region.

2) Metallic bead

$\varepsilon_r \to \infty$: $\mu_r \to 0$ (diamagnetic due to the induced currents)

$$\frac{\Delta\omega}{\omega} = -\frac{\pi r_1^3}{U}\left[\varepsilon_o E_{ou}^2 - \frac{\mu_o}{2}H_{ou}^2\right].$$

The magnetic field term increases the stored energy! The metallic bead measures E_{ou} and H_{ou}. In order to separate these contributions, two measurements are needed (metallic + dielectric bead).

Instead of perturbing spheres, ellipsoids of revolution can be used, the depolarization factor N will then change:

$$\begin{aligned} &\text{sphere:} && N = \frac{1}{3} \\ &\text{oblate ellipsoid:} && \frac{1}{3} < N < 1 \\ &\text{prolate ellipsoid:} && 0 < N < \frac{1}{3} . \end{aligned}$$

With ellipsoids the field direction can be determined. Furthermore, for a metallic needle the effect of the parallel electric field is much larger than that of the magnetic field or of a perpendicular electrical field which can be advantageous in many practical cases.

Other geometries are to be considered with caution (e.g. a metallic cylinder), since the fields are rather complicated and may no longer be homogeneous inside. To get precise results, the perturbating ball should be calibrated in a resonator with a known field distribution [8]. In a normal setup for perturbation measurements the bead is moved through the cavity. But the mechanical oscillations of the bead make it difficult to define its position exactly, especially in small resonators used at high frequencies. In that case, the bead is kept stationary and the cavity is moved. $\Delta\omega$ can be measured directly, or by the change in phase corresponding to the measurement of Q.

Consider as an easy example a rectangular cavity (see Fig. 13). This is effectively a section of a rectangular waveguide, short circuited at both ends with flat parallel plates. The fields are described and shown below in the equations and figures 13 and 14.

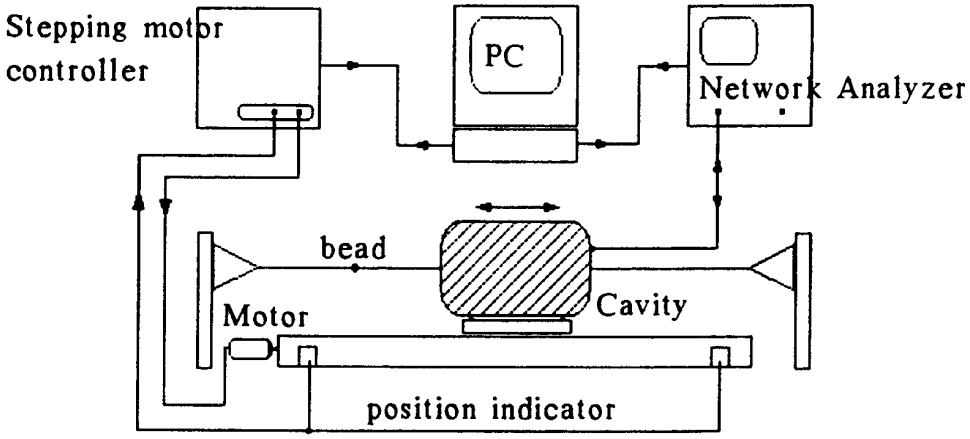

Fig. 12 Test bench for perturbation measurements at high frequencies

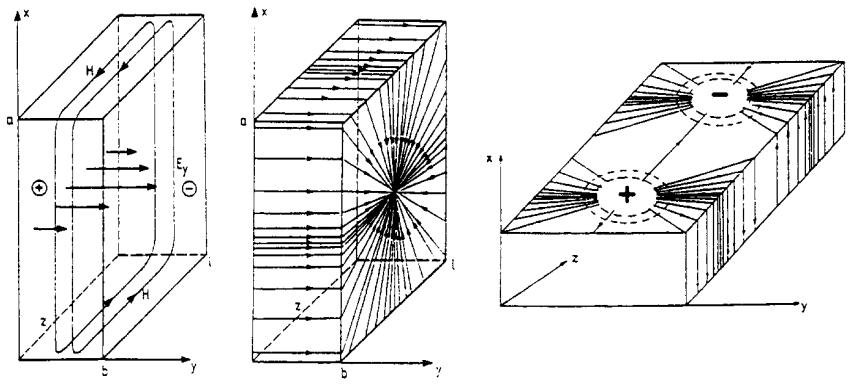

Fig. 13 Diagrammatic view of fields in a rectangular cavity

TE-*modes in rectangular cavity*

$$E_x = -i\frac{\omega\mu_o}{k_c^2} H_o \frac{n\pi}{b} cos\left(\frac{m\pi x}{a}\right) sin\left(\frac{n\pi y}{b}\right) sin\left(\frac{s\pi z}{1}\right)$$

$$E_y = i\frac{\omega\mu_o}{k_c^2} H_o \frac{m\pi}{a} sin\left(\frac{m\pi x}{a}\right) cos\left(\frac{n\pi y}{b}\right) sin\left(\frac{s\pi z}{1}\right)$$

$$E_z = 0$$

$$H_x = -\frac{m\pi}{a}\frac{s\pi}{1}\frac{1}{k_c^2} H_o sin\left(\frac{m\pi x}{a}\right) cos\left(\frac{n\pi y}{b}\right) cos\left(\frac{s\pi z}{1}\right)$$

$$H_y = -\frac{n\pi}{a}\frac{s\pi}{1}\frac{1}{k_c^2} H_o cos\left(\frac{m\pi x}{a}\right) sin\left(\frac{n\pi y}{b}\right) cos\left(\frac{s\pi z}{1}\right)$$

$$H_z = H_o cos\left(\frac{m\pi x}{a}\right) cos\left(\frac{n\pi y}{b}\right) sin\left(\frac{s\pi z}{1}\right)$$

$s \neq 0$ m or n may be zero

$$r_{res} = \frac{c}{2\pi}\sqrt{\left(\frac{\pi m}{a}\right)^2 + \left(\frac{\pi n}{b}\right)^2 + \left(\frac{\pi s}{1}\right)^2} \quad .$$

TE_{101}-*mode in rectangular cavity*

$$m = 1, \quad n = 0, \quad s = 1, \quad y = b/2, \quad z = 1/2$$

$$E_x = E_z = H_x = H_y = 0$$

$$E_y = iE_{oy} \sin\left(\frac{\pi x}{a}\right)$$

$$H_z = H_{oz} \cos\left(\frac{\pi x}{a}\right).$$

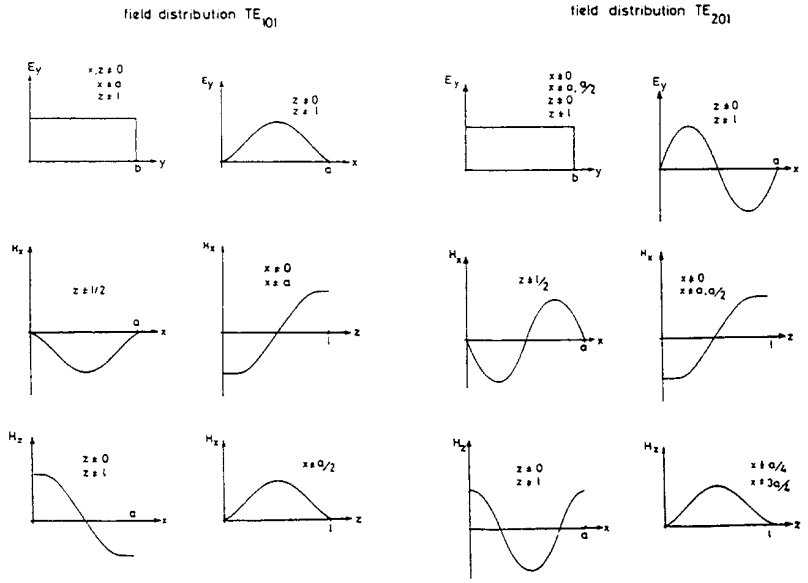

Fig. 14 Field distributions for TE_{101} and TE_{201} modes

The results of a typical measurements using the equipment in Fig. 12 is shown in Fig. 15.

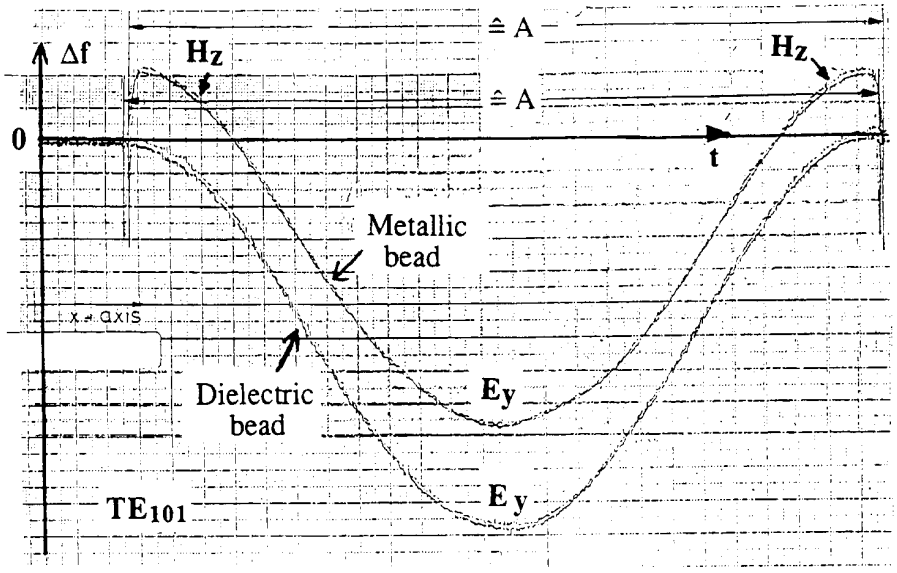

Fig. 15 Frequency perturbation measurements with dielectric and metallic beads

Placing the bead near the cavity walls should be avoided since the mirror fields influence the results. For example, in the case of a dielectric bead $\Delta\omega$ will be increased. The field in the perturbating dielectric sphere will change from

$$E_1 = \frac{3}{\varepsilon_r t^2} E_u \quad \text{to} \quad E_i = \frac{3}{(\varepsilon_r + 2) - \frac{1}{4}(\varepsilon_r - 1)\left(\frac{r_1}{d}\right)^3} E_u$$

where r_1 is the radius of the sphere and d is the distance of the centre of the bead to the wall. This results in [9]:

$$\frac{\Delta\omega}{\omega} = -\frac{\pi r_1^3}{W}\varepsilon_o \frac{\varepsilon_r - 1}{(\varepsilon_r + 2) - \frac{1}{4}(\varepsilon_r - 1)\left(\frac{r_1}{d}\right)^3} E_{ou}^2 .$$

Theory and measurement show that for distances $d \geq 2r_1$ the mirror dipole effects are negligible.

4. NONRESONANT PERTURBATION THEORY

Measurement of both the electric and magnetic fields in an arbitrary cavity can be performed by measuring the change in the reflection coefficient $\rho = |\rho| e^{i\phi}$ at a test port while a bead is pulled through the cavity [10-11]. The requirements for this type of measurement are:

(i) No energy can leave or enter the cavity apart via the test port.
(ii) Only one mode is present at the test port.
(iii) Operating frequency is left constant during measurements.
(iv) Losses occur inside the cavity and materials used are linear and isotropic.
(v). The surface S lies inside the cavity walls, except for the test port (see Fig. 16).

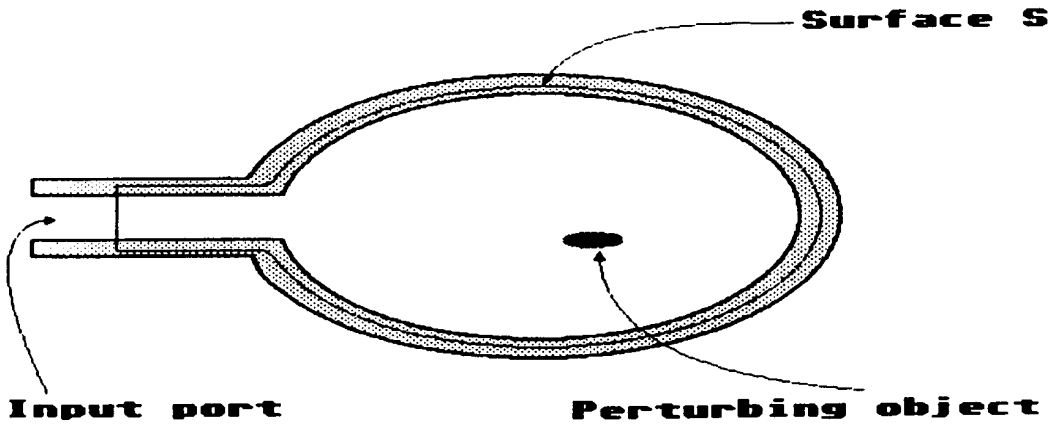

Fig. 16 Schematic picture for nonresonant perturbation theory

Similarly to the Lorentz Reciprocity Theorem, a vector $\vec{p}$ can be introduced with the definition of

$$\vec{p} = \vec{E}_u \times \vec{H}_p - \vec{E}_p \times \vec{H}_u \qquad (73)$$

where subscript u denotes the unperturbed fields and p the perturbed fields. Choose the enclosing surface S such that there is a surface S_2 for which

$$\vec{E}_u = \vec{H}_u = \vec{E}_p = \vec{H}_p = \vec{p} = 0 \tag{74}$$

and a surface S_1 (at the test port), where the fields are not zero, so that

$$\int_S (\vec{p}\vec{n})\ ds\ = \int_{S_1} (\vec{p}\vec{n})\ ds\ . \tag{75}$$

Over surface S_1:

$$\vec{p}\vec{n} = \vec{n}\left(\vec{E}_u \times \vec{H}_p\right) - \vec{n}\left(\vec{E}_p \times \vec{H}_u\right) \Rightarrow \vec{p}\vec{n} = E_{ps}H_{us} - E_{us}H_{ps} \tag{76}$$

where the subscript s denotes a direction parallel to S_1. Expressing the fields as

$$\begin{aligned} E_{us} &= (1+\rho_u)E_{usi}, \quad H_{us} = (1-\rho_u)H_{usi} \\ E_{ps} &= (1+\rho_p)E_{psi} \quad H_{ps} = (1-\rho_p)H_{psi} \end{aligned} \tag{77}$$

where the subscript i denotes incident waves and ρ_u, ρ_p are reflection coefficients, then

$$\int_{S_1} (\vec{p}\vec{n})\ ds\ = (\rho_p - \rho_u)\int_{S_1} \left(E_{usi}H_{psi} + E_{psi}H_{usi}\right)\ ds\ . \tag{78}$$

As the power flow into the cavity is kept constant, the incident fields are of the same value in either case, so that

$$\int_{S_1} (\vec{p}\vec{n})\ ds\ = 2P_i(\rho_p - \rho_u)\ . \tag{79}$$

On the other hand

$$\int_{S_1} (\vec{p}\vec{n})\ ds\ = \int_{S_1} \left(E_{ps}H_{us} - E_{us}H_{ps}\right)\ ds\ . \tag{80}$$

If the perturbing object is assumed to be small compared to the wavelength, its scattered fields will be of almost a pure dipole-type and E_{ps} and H_{ps} can be expressed as

$$E_{ps} = E_{ds} + E_{us} \quad H_{ps} = H_{ds} + H_{us}$$

where the subscript d denotes the dipole part of the fields. Thus

$$2P_i(\rho_p - \rho_u) = \int_{S_1} \left(E_{ds}H_{ds} - E_{us}H_{ds}\right)\ ds\ . \tag{81}$$

Writing E_{ds}, H_{ds} in terms of the dipole moments set up by the object gives

$$\begin{aligned} E_{ds} &= \vec{C}_1\vec{P} + \vec{C}_2\vec{M} \qquad\qquad H_{ds} = \vec{C}_3\vec{P} + \vec{C}_4\vec{M} \\ 2P_i(\rho_p - \rho_u) &= K_1\vec{P} + K_2\vec{M} \end{aligned} \tag{82}$$

where

$$K_1 = \int_S \left(\vec{H}_{us}\vec{C}_1 - \vec{E}_{us}\vec{C}_3\right)\, ds$$

$$K_2 = \int_S \left(\vec{H}_{us}\vec{C}_2 - \vec{E}_{us}\vec{C}_4\right)\, ds\ . \tag{83}$$

The assumption of ideal electrical and magnetic dipoles (by using the Reciprocity Theorem and comparing coefficients) leads to

$$K_1 = -i\omega E_u \quad K_2 = i\omega\mu_o H_u$$

$$\text{and hence}\quad 2P_i\left(\rho_p - \rho_u\right) = -i\omega\left(\vec{E}_u\vec{P} - \mu_o\vec{H}_u\vec{M}\right) \tag{84}$$

with

$$\vec{P} = \varepsilon_o\alpha_e\vec{E}_u \quad \text{(isotropic materials)}$$

$$\vec{M} = \alpha_m\vec{H}_u\ . \tag{85}$$

the final result is

$$2P_i\left(\rho_p - \rho_u\right) = -i\omega\left(\varepsilon_o\alpha_e\vec{E}_u^2 - \mu_o\alpha_m\vec{H}_u^2\right)\ . \tag{86}$$

For a dielectric and magnetic beads of radius r_1

$$\alpha_e = 4\pi r_1^3\,\frac{\varepsilon_r - 1}{\varepsilon_r + 2}\ , \qquad \alpha_m = 4\pi r_1^3\,\frac{\mu_r - 1}{\mu_r + 2}\ . \tag{87}$$

In order to determine both the electric and magnetic fields, two successive measurements are required with dielectric and magnetic (e.g. metal) beads as perturbing objects (as in the resonant case). For this more general "nonresonant" method it is unimportant whether the cavity is in resonance or not!

5. SHUNT IMPEDANCE R_S, R_S/Q

An important quantity to characterize the effectiveness of an rf driven accelerating gap is its "shunt impedance", as defined by

$$R_S = \frac{V_o^2}{2W} \tag{88}$$

where qV_o is the energy gain of a particle with charge q traversing the gap at optimum phase, and W is the power dissipated in the associated metal surfaces. The factor 2 in the denominator is applied to keep the analogy to Ohm's law $V^2_{\text{eff}} = R{\cdot}W$, with $V_{\text{eff}} = V_o/\sqrt{2}$.

Consider now a row of length L of n equal gaps. Its energy gain is

$$\Delta T_o = q\cdot\sqrt{2R_SW}\cdot n \tag{89}$$

By introducing a "mean accelerating field" E_0 defined by $E_0 = \Delta T_0/qL$ we have

$$E_o = \sqrt{2R_S W} \cdot \frac{n}{L} = \sqrt{2\frac{R_S n}{L} \cdot \frac{W_n}{L}} = \sqrt{2R_S' W'} \tag{90}$$

where W is the power dissipated per unit length and R'_S the shunt impedance per unit length, which is commonly used to quantify the effectiveness of an accelerating structure

$$R_S' = \frac{E_o^2}{2W'} \tag{91}$$

Actually, the V_0 and E_0 used in Eqs. (88) and (90) have to be evaluated using the axial field "seen" by the particle, i.e.

$$V_o = \int_{-\infty}^{+\infty} E(z,t(z))dz \quad \text{or} \tag{92}$$

$$E_o = \frac{1}{L}\int_0^L E(z,t(z))dz \quad \text{resp.} \tag{93}$$

where $E(z,t)$ is the axial electric field as a function of space and time and $t(z)$ is the time, at which a particle is at location z, i.e. $t(z) = \int dz/v + t_0$, where t_0 has to be chosen such that the integral (which is quite generally proportional to cos ωt) becomes maximum.

Obviously, if the particles have to be accelerated off this optimum phase (which is usually the case for reasons of beam dynamics) the actual accelerating field is

$$E = E_o \cdot \cos\phi_S \sqrt{2R_S' W'} \tag{94}$$

where $\phi_S = \omega(t_S - t_0)$ is the phase angle by which the particle differs from ωt_0.

Equations (92) and (93) may be illustrated by simple special cases:

In Eq. (92), if the traversing time is very short compared to the rf period, V_0 becomes simply the voltage along the gap.

In Eq. (93), $E(z,t) = A\cos(\omega t - kz)$, i.e. $E(z,t)$ is a travelling wave with phase velocity $v = \omega/k$ E_0 is equal to the amplitude A of the travelling wave.

The value of the electric field strength depending on z can be measured by using the perturbation method with an electric sphere (Eq. (72)), and the mean value of the electric field is then given by:

$$E_o = \frac{1}{L}\int_0^L E(z)dz = \frac{1}{L\omega_o}\sqrt{\frac{\omega Q}{\pi r_1^3}\frac{\varepsilon_r + 2}{(\varepsilon_r - 1)\varepsilon_o}}\int_0^L \sqrt{\Delta\omega}dz \tag{95}$$

The time dependence of E has to be considered by a so-called transit time factor separately, this factor is implicitly contained in Eq. (92).

Also often used is the ratio of shunt impedance (88) and the quality factor (38):

$$\frac{R_S}{Q} = \frac{V_o^2}{2\omega U} \tag{96}$$

Since $U \sim V^2_0$, this expression only depends on the cavity geometry; it allows, for example, the comparison of the effectiveness of different structures.

6. MEASUREMENT OF THE POTENTIAL DIFFERENCE V IN RF GAPS

Having measured the electrical field as a function of location, V is then given by $V = \int E \cdot d\ell$. But in cases of complicated structures like RFQ, where the precise measurement of E is difficult, it is convenient to measure the field between two tubes, which are connected to the electrodes, between which V shall be determined. This can be done easily by bead measurement through the gap (see Fig. 17) [12]. The drift tubes must not disturb the original field distribution and the resonance frequency, their capacitance therefore has to be sufficiently small.

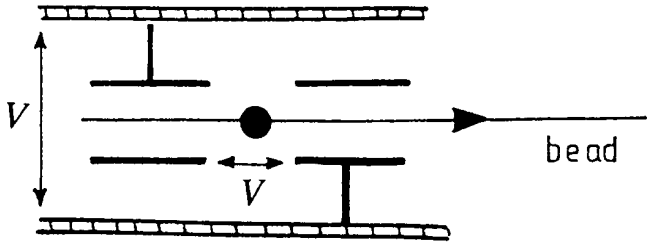

Fig. 17 Measurement of potential difference V

If an accelerator cavity is operated at high power level, another method gives astonishingly precise results (0.5-5% depending on experimental setup) by measuring the X-ray spectrum. The spectrum originates from electrons (always present due to field emission and background radiation) accelerated in the gaps. The highest energy which they can get is $V \cdot e$, V being the maximum voltage between the electrodes. This technique is applicable for voltages exceeding about 40 kV for a standard n-type Ge detector. An example is given in Fig. 18. The X-ray spectrum ends at 243 keV. Since the X-ray detector was shielded by lead, the spectrum also shows the characteristic X-ray peaks for Pb. In all measurements, absorbers (useful are Al, Cu, Sn, Pb depending on voltage) have to be used to cut the uninteresting low-energy part of the bremsstrahlung spectrum and to reduce X-ray intensity on the detector [13]. By moving the shielded detector the voltage distribution along the accelerator can be scanned.

ACKNOWLEDGEMENTS

For valuable discussions and especially for the hints on the nonresonant perturbation method I would like to thank Professor Dr. H. Herminghaus, Institut für Kernphysik, University of Mainz. My thanks go also to Dipl. Phys. P. Hülsmann and Dipl. Phys. M. Kurz, Institut für Angewandte Physik, University of Frankfurt for many discussions and their contributions to this chapter. Furthermore the author is very much indebted to P.J. Bryant, W. Hardt, and S. Turner (CERN) for their very valuable help and support in finishing the manuscript.

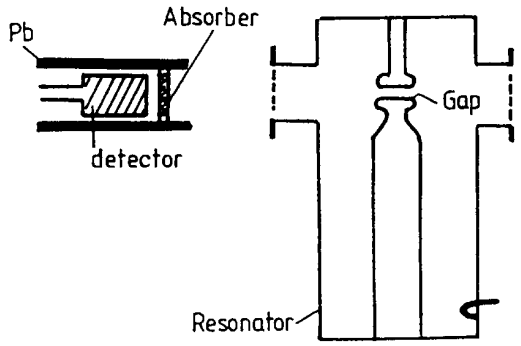

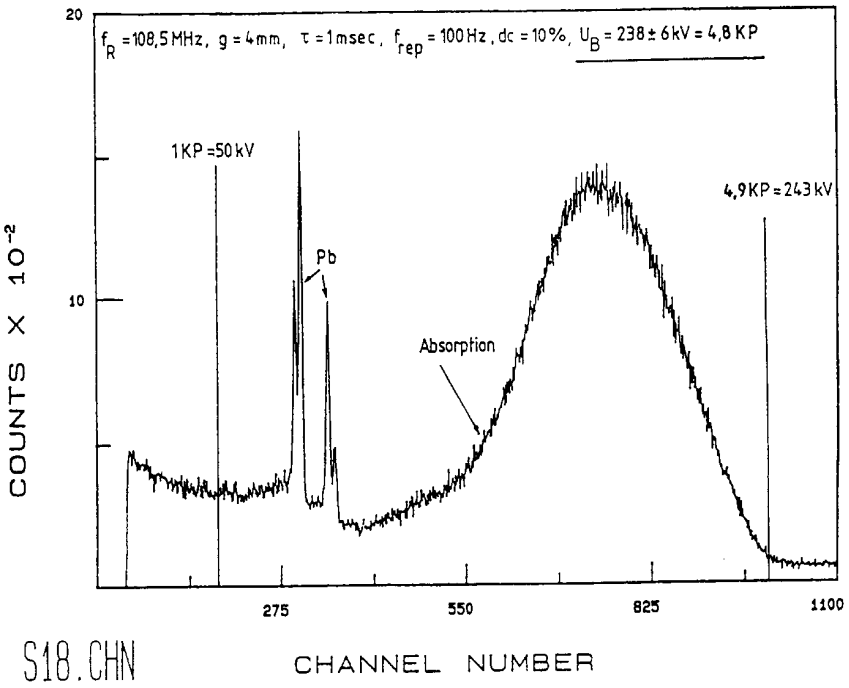

Fig. 18 X-ray spectrum in a cavity

REFERENCES

[1] L. Boltzmann, Vorlesungen über Mechanik II, Leipzig, J.A. Barth, 1904.

[2] P. Ehrenfest, Annalen der Physik, Vol. 36, 1991.

[3] P. Ehrenfest, Proceedings of Amsterdam Academy, Vol. 16, 1914.

[4] W.R. Maclean, The Resonator Action Theorem, Quarterly of Applied Mathematics, Vol. 2, 1945.

[5] L.C. Maier and J.C. Slater, Field Strength Measurements in Resonant Cavities, Journal of Applied Physics, Vol. 23, Nr. 1, 1952.

[6] L.C. Maier and J.C. Slater, Determination of Field Strength in a Linear Accelerator Cavity, Journal of Applied Physics, Vol. 23, Nr. 1. 1952.

[7] E. Müller, Untersuchungen zur Feldmessung und Hochfrequenzankopplung bei Spiralresonatoren, Diplomarbeit, Institut für Angewandte Physik, Frankfurt am Main, 1977.

[8] F. Caspers and G. Dome, Precise Perturbation Measurements of Resonant Cavities and Higher Order Mode Identification, CERN SPS/85-46 (ARF), 1985.

[9] W. Saunders, Measurement of Electromagnetic Parameters by Use of Spheres Placed Near a Wall in a Resonant Cavity, I.R.E., Convention Record, Vol. 8., 1955.

[10] C.W. Steele, A. Nonresonant Perturbation Theory, IEEE Transaction on Microwave Theory and Techniques, Vol. MTT-14, No. 2, 1966.

[11] H. Süss, Aufbau einer Apparatur zur Ausmessung laufender elektrischer Wellen und ihre Benutzung zur Dimensionierung einer Bunchersektion, Diplomarbeit, Institut für Kernphysik, Mainz, 1977.

[12] A. Schempp, Four-Rod-RFQ-R_p-Messung, Institut für Angewandte Physik, Int. Rep. 87-12, 1987.

[13] J. Brutscher, A. Gerhard, H. Klein, M. Kurz, A. Schempp, Measurements of the Gap Voltage in RF Cavities by Using an X-Ray Spectrometer, Institut für Angewandte Physik, Frankfurt am Main, GSI-Report 88-17, 1988, S. 34.

BIBLIOGRAPHY

J.C. Slater, Microwave Electronics, D. Van Nostrand Comp., Princeton.

P. Lapostolle and A. Septier, Linear Accelerators, North-Holland Publishing Comp., Amsterdam.

E.L. Ginzton, Microwave Measurements, McGraw-Hill Book Comp., New York.